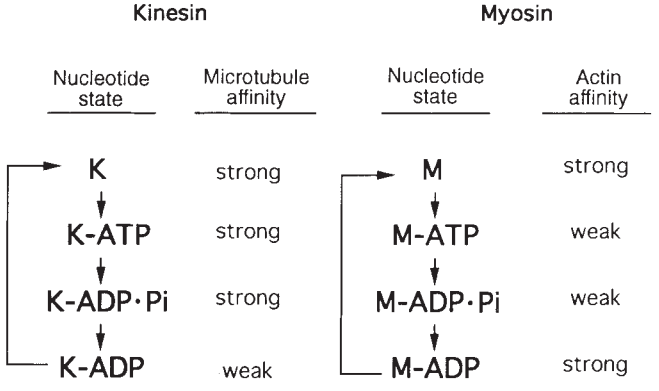

FIG. 3 Models for the filament binding interactions of kinesin (K) and myosin (M) during the ATP hydrolysis cycle. Possibilities of multiple nucleotide states or mechanical influence are not included in this scheme.

ADP caused microtubules to dissociate from single kinesins twice as frequently; no binding was detected with 250 μM ADP (Table 1). Similar concentrations of ADP in the absence of ATP also dissociated microtubules from kinesin (data not shown). These results suggest that ADP weakens the binding between kinesin and microtubules. The sudden suppression of translocation with increasing ADP may reflect the need for both kinesin heads to detach simultaneously in order for a microtubule to dissociate. Consistent with this idea, higher concentrations of ADP (5–20 mM) were required to dissociate microtubules in the multiple motor assay.

These results suggest the following sequence of interactions between kinesin and microtubules during the ATP hydrolysis cycle (Fig. 3). In the nucleotide-free state, kinesin is strongly bound to microtubules. After nucleotide binding, the motor remains tightly associated with the polymer, yet some conformational change must occur that diminishes its ability to resist microtubule translocation in a multiple motor assay. Kinesin-ADP·Pi is still strongly bound to the microtubule, but after phosphate release, the interaction becomes weak, potentially allowing the motor to dissociate and find a new binding site. This model of the kinesin cycle requires the assumption that the analogues and inhibitors used here prolong the predicted states and that these states mimic normal intermediates in hydrolysis. Transient-state kinetic measurements[13,14] of kinesin dissociation during the normal ATPase cycle will be needed to confirm this model.

In a motor protein's chemomechanical cycle, energy is required to dissociate the strongly bound motor–polymer complex and to produce force. Our results suggest that the utilization of ATP energy by kinesin is different from that of other cytoskeletal motors. Upon binding ATP, myosin[13] and dynein[14,15] rapidly dissociate from their filaments. Although the binding of ATP to kinesin is associated with a free energy change[16] of similar magnitude to that of other motors[17,18], our results indicate that kinesin does not dissociate from microtubules early in its hydrolysis cycle. How then does kinesin use the binding energy of ATP? One possibility is that the energy may be stored in the protein for use later in the cycle, as occurs for other proteins such as bacteriorhodopsin[19]. Alternatively, the binding of ATP may be directly coupled to mechanical work. This issue can be resolved by determining when force production occurs in the hydrolysis cycle. □

Received 28 September; accepted 2 November 1992.

1. Eisenberg, E. & Hill, T. L. *Science* **227,** 999–1006 (1985).
2. Jencks, W. P. in *The Roots of Modern Biochemistry* 571–580 (Walter de Gruyer, Berlin, 1988).
3. Cooke, R. *CRC crit. Rev. Biochem.* **21,** 53–118 (1986).
4. Johnson, K. A. *A. Rev. Biophys. biophys. Chem.* **14,** 161–188 (1985).
5. Howard, J., Hudspeth, A. J. & Vale, R. D. *Nature* **342,** 154–158 (1989).
6. Block, S. M., Goldtein, L. S. & Schnapp, B. J. *Nature* **348,** 348–352 (1990).
7. Hackney, D. D. *Proc. natn. Acad. Sci. U.S.A.* **85,** 6314–6318 (1988).
8. Pate, E. & Cooke, R. *J. Musc. Res. Cell Motil.* **12,** 376–393 (1991).
9. Kuznetsov, S. A. & Gelfand, V. I. *Proc. natn. Acad. Sci. U.S.A.* **83,** 8350–8354 (1986).
10. Goody, R. S. & Mannherz, H. G. in *Protein–Ligand Interactions* (eds Sund, H. & Blauer, G.) (Walter de Hruyer, Berlin, 1975).
11. Shimizu, T., Katsura, T., Domanico, P. L., Marchese-Ragona, S. P. & Johnson, K. A. *Biochemistry* **28,** 7022–7027 (1989).
12. Cohn, S. A., Ingold, A. L. & Scholey, J. M. *J. biol. Chem.* **264,** 4290–4297 (1989).
13. Lymm, R. W. & Taylor, E. W. *Biochemistry* **10,** 4617–4624 (1971).
14. Porter, M. E. & Johnson, K. A. *J. biol. Chem.* **258,** 6582–6587 (1983).
15. Omoto, C. K. & Johnson, K. A. *Biochemistry* **25,** 419–427 (1986).
16. Sadhu, A. & Taylor, E. W. *J. biol. Chem.* **267,** 11352–11359 (1992).
17. Taylor, E. W. in *Heart and Cardiovascular System* (eds Fozzard, H. A.) 1281–1293 (Raven, New York, 1992).
18. Holzbaur, E. L. F. & Johnson, J. A. *Biochemistry* **25,** 428–434 (1986).
19. Mathies, R. A., Lin, S. W., Ames, J. B. & Pollard, W. T. *A. Rev. Biophys. Chem.* **20,** 491–518 (1991).
20. Vale, R. D., Reese, T. S. & Sheetz, M. P. *Cell* **42,** 39–50 (1985).

ACKNOWLEDGEMENTS. We thank F. Malik for purifying kinesin, T. Shimizu and T. Mitchison for advice on purification of ATP-γS, W. Marshall for developing the measurement program, R. Cooke for discussion, and F. Malik, G. McCaffrey and F. McNally for critically reading the manuscript. This work was supported by a grant from the NIH.

A role for reverse transcripts in gene conversion

Leslie K. Derr & Jeffrey N. Strathern

Laboratory of Eukaryotic Gene Expression, NCI Frederick Cancer Research and Development Center, Frederick, Maryland 21702, USA

RECOMBINATION between a diffusible reverse transcript and its homologous chromosomal allele has been proposed as a mechanism for the precise removal of introns from DNA and gene conversion of dispersed repeated sequences[1,2]. We have reported that RNA-mediated recombination occurs in the yeast *Saccharomyces cerevisiae*[3]. This recombination requires expression of the retrotransposon Ty, and results in intron loss from a plasmid-borne marker gene and the formation of pseudogenes. Because the pseudogenes are embedded in Ty sequences, chromosomal insertion could have been mediated by Ty integrase or by homologous recombination with endogenous Ty sequences. The structure of the chromosomal recombinants and the fact that plasmid and chromosomal recombination can have different requirements demanded a direct demonstration of RNA-mediated gene conversion of a chromosomal allele. Here we report the first demonstration, to our knowledge, of recombination between a reverse transcript and its chromosomal homologue and describe an assay that specifically detects this novel recombination pathway.

To address the question of whether RNA-mediated recombination can contribute to mitotic gene conversion, we generated a system specifically to monitor chromosomal RNA-mediated events. This system has as its essential features a plasmid donor of complementary DNA and a homologous chromosomal target. The plasmid (Fig. 1*a*) carries a *his3* reporter gene whose coding sequence is interrupted by an artificial intron. The intron is inserted at a unique *Msc*I site, in an unspliceable orientation relative to the *HIS*3 promoter. Induction from a *GAL1* promoter fused to the 3′ end of *his3* produces a spliceable transcript. Reverse transcription of this spliced antisense *his3* transcript can lead to $His3^+$ prototrophy in a strain containing a chromosomal *his3* deletion (*his3-Δ200*)[3]. To provide a homologous chromosomal target, a 34-base-pair (bp) deletion spanning the *Msc*I site of *his3*, *his3-ΔMscI*, was inserted at the *MAT* locus on chromosome III. DNA recombination between plasmid and chromosomal *his3* sequences cannot generate a *HIS3* allele. $His3^+$ prototrophs can result from recombination between the *HIS3* cDNA and chromosomal *his3-ΔMscI* allele (Fig. 1*d*).

Because the presence of a homologous chromosomal target might increase the rate of formation of chromosomal $His3^+$

© 1993 Nature Publishing Group

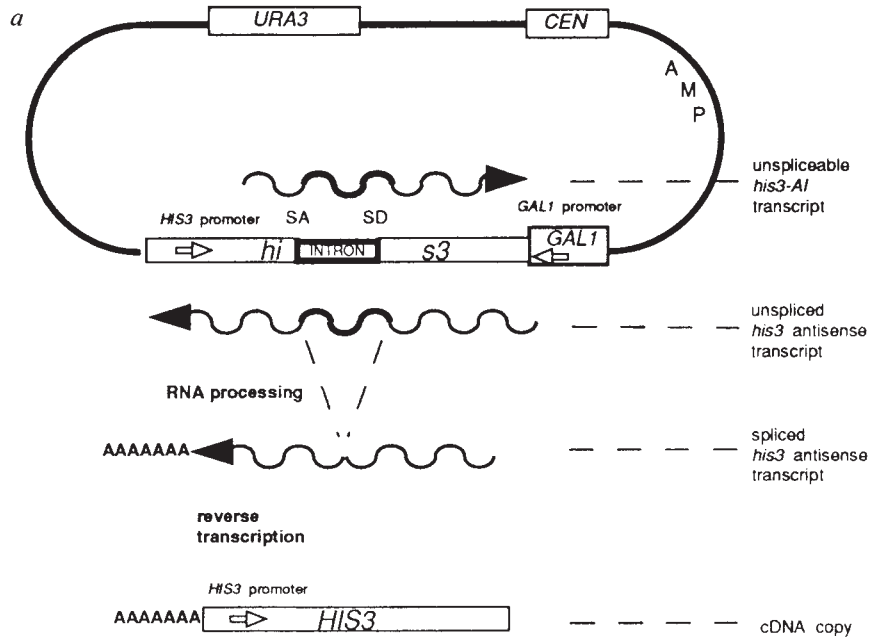

FIG. 1 An assay for RNA-mediated recombination and the resultant products. *a*, The *GAL1-his3-AI* plasmid acts as the donor of *HIS3* cDNA. The yeast *his3* gene is interrupted by an artificial intron inserted into a unique *Msc*I site in the unspliceable orientation relative to the *HIS3* promoter, but in the spliceable orientation relative to the *GAL1* promoter. Transcripts are shown as wavy lines and the presence of the intron is indicated by thicker lines. SD, splice donor; SA, splice acceptor. The formation of *HIS3* cDNA requires reverse transcription of the spliced antisense *his3* transcript. This cDNA is then involved in a subsequent recombination event. *b*, RNA-mediated gene conversion of plasmid *his3-AI* sequences, resulting in loss. *c*, Insertion into a chromosome in the absence of *his3* homology, resulting in cDNA gene formation. J3, 3′ junction and J5, 5′ junction: previous analyses have shown these junction sequences to be Ty sequences, the orientation and extent of Ty sequences present varies[3] *d*, RNA-mediated gene conversion of chromosomal *his3* sequences. Chequered sequences are chromosomal sequences; stippling indicates a deletion mutation.

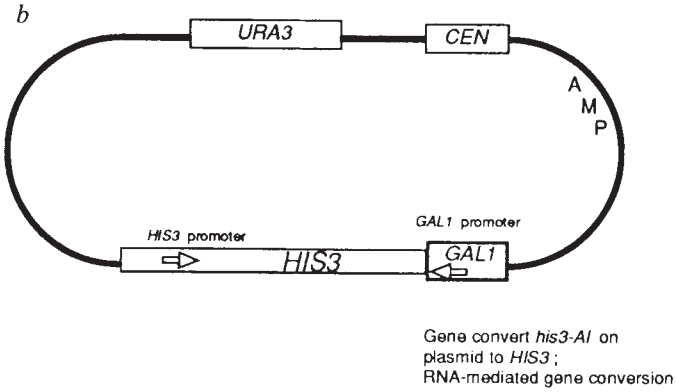

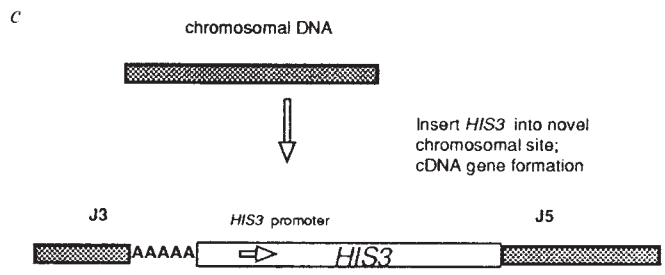

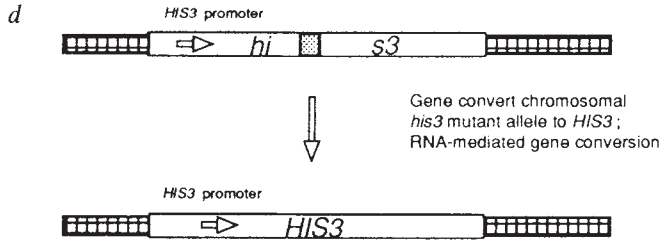

recombinants, we compared the rate of $His3^+$ prototroph formation in a strain lacking chromosomal *his3* homology (*his3-Δ200*) with a strain containing *his3-ΔMscI* target sequences (*his3-Δ200, MAT::his3-ΔMscI*). As seen in Table 1 (compare L1890 with YLD125), the rate of $His3^+$ prototroph formation was not increased by the presence of chromosomal *his3* homology, nor was the proportion of events that were chromosomal increased by providing a *his3* target. Therefore, the rate of formation of chromosomal $His3^+$ prototrophs is not limited by *his3* homology.

We then asked how often chromosomal $His3^+$ prototrophs are the result of recombination with *his3-ΔMscI* target sequences. The most direct test of this was to assay for the presence of a 1-kilobase (kb) polymerase chain reaction (PCR) product that could only result if *HIS3* were linked to *MAT* (Fig. 2). Using one primer complementary to *HIS3* sequences spanning the *Msc*I site (deleted in *his3-ΔMscI*) and the other complementary to *MAT* sequences, we determined that 5/75 independent chromosomal $His3^+$ prototrophs had been targeted to *his3-ΔMscI* sequences at *MAT* (Table 2).

Because a *rad52* mutation reduces mitotic recombination[4], we measured $His3^+$ prototroph formation in a *rad52*-mutant background. If we first consider RNA events mediated by *his3* homology, we found 0/92 independent chromosomal $His3^+$ prototrophs linked to *MAT* (Table 2). The proportion of plasmid events was also reduced relative to the wild type. But plasmid events were observed, indicating that this homologous recombination event has a *RAD52*-independent component (Table 1). Overall, the rate of $His3^+$ prototroph formation was not affected by the *rad52* mutation (Table 1). These results suggest that a *rad52*-independent mechanism of chromosomal insertion also exists. The simplest explanation, based on the structure of the chromosomal $His3^+$ prototrophs, is that insertion is mediated by Ty integrase[3] (see above).

The experiments described above suggested that at least three pathways existed for the insertion of *HIS3* cDNA: insertion by Ty integrase, *RAD52*-dependent gene conversion (plasmid and chromosomal events) and *rad52*-independent gene conversion (plasmid events only). To eliminate plasmid events and those events mediated by Ty integrase, the *HIS3* promoter and the initiation codon of the plasmid *his3-AI* sequences were deleted, generating a plasmid-borne *his3-ΔATG* allele. No ($0/1.5\times10^{10}$) $His3^+$ events were observed in a *his3-Δ200* strain. But $His3^+$ prototrophs were observed at a rate of 2.0×10^{-9} when RNA-mediated recombination with chromosomal *his3-ΔMscI* sequences was possible (Table 2). This 10-fold decrease in the rate of

© 1993 Nature Publishing Group

TABLE 1 Rate of $His3^+$ prototroph formation

Strain chromosomal *his3* allele(s)	Rate ($\times10^{-8}$)	*RAD52*	Chromosomal (%)
L1890 *his3-Δ200*	3.1	*RAD52*	53 (39/73)
YLD125 *his3-Δ200, his3-ΔMscI*	1.8	*RAD52*	53 (40/75)
YLD117 *his3-Δ200*	3.2	*rad52*	77 (57/74)
YLD157 *his3-Δ200, his3-ΔMscI*	3.9	*rad52*	75 (64/86)

Genotype of strains: L1890 (*MAT***a** *his3-Δ200 ura3-52 trpl-289 lys*); YLD125 (*MAT***a**::*his3-ΔMscI his3-Δ200 ura3-52 trpl-289 lys*); YLD117 (*MAT***a** *his3-Δ200 ura3-52 trpl-289 lys rad52-542*); YLD157 (*MAT***a**::*his3-ΔMscI his3-Δ200 ura3-52 trpl-289 lys rad52-542*). These isogenic strains carry the *URA3*-marked, CEN-based, *GAL1-his3-AI* plasmid. Rates were computed by the method of Lea and Coulson[9] from the median tube in 75 (*RAD52*) and 100 (*rad52-542*) tube experiments. Isogenic strains carrying the *GAL1-his3-AI* plasmid were grown to saturation in media lacking uracil and containing galactose at 20 °C, and then scored on plates lacking histidine, with incubation at 30 °C. One $His3^+$ event was picked randomly from each culture and chromosomal events were distinguished from plasmid events by selecting for loss of the plasmid (Ura^-) by plating on FOA (ref. 10). Chromosomal events have a Ura^- His^+ phenotype. The *rad52-542* allele was made by the method of Alani *et al.*[11]. The *rad52-542* mutation was confirmed by MMS^S and Southern analysis (data not shown). The proportion of events that are chromosomal depending on the allele state of *RAD52* is significant at $\chi^2=6.11$, $P<0.025$.

$His3^+$ prototroph formation corresponds nicely with the 3.5% ($0.53\times5/75$) $His3^+$ prototrophs linked to *MAT*. As expected, all of the $His3^+$ prototrophs were gene convertants of the *his3-ΔMscI* allele. This assay provides a means of assaying the cellular proteins specifically involved in recombination between a cDNA and its chromosomal allele.

RNA-mediated recombination offers a distinct pathway for gene conversion of chromosomal alleles. Spontaneous mitotic recombination between *his3* heteroalleles occurs at a 100-fold higher rate than RNA-mediated gene conversion[5]. To compare these RNA and 'DNA' rates, one should note that the alleles are different, but more importantly that the transcripts that can serve as potential donors are different. If the spontaneous events use an RNA-mediated pathway, then they act on the sense strand as opposed to the antisense *his3* strand. Additionally, the level of *his3* expression is different, the transcript produced here is from the efficient *GAL1* promoter, not the *HIS3* promoter. Any feature affecting the transcript, such as its abundance and its ability to serve as a substrate for reverse transcription, necessarily influences the rate of RNA-mediated recombination.

TABLE 2 RNA-mediated gene conversion of chromosomal *his3-ΔMscI* sequences

Strain (*RAD52*)	Plasmid	Rate ($\times10^{-8}$)	Chromosomal $HIS3^+$ prototrophs linked to *MAT*
YLD125 (*RAD52*)	*GAL1-his3-AI*	1.8	5/75
YLD157 (*rad52*)	*GAL1-his3-AI*	3.9	0/92
YLD125* (*RAD52*)	*GAL1-his3-ΔATG*	0.2	52/52

Strains are as in Table 1. Rates were computed as in Table 1. Chromosomal events were distinguished as in Table 1 and one chromosomal event was then picked from each culture. Independent (except for *GAL1-his3-ΔATG* see footnote below) chromosomal $His3^+$ prototrophs were analysed to determine the linkage of *HIS3* and *MAT*. $His3^+$ events linked to *MAT* were identified by the presence of a 1-kb PCR product and genetic linkage analysis. The observation that no $His3^+$ prototrophs are linked to *MAT* in *rad52-542* background is significant at $\chi^2=5.84$, $P<0.025$.

* The *his3-ΔATG* mutation was created using PCR, resulting in the deletion of *HIS3* nucleotides $-172\rightarrow+27$ (ref. 12). Nine cultures, inoculated with 10^4 cells containing the *GAL1-his3-ΔATG* plasmid were grown to saturation in media lacking uracil and containing galactose at 20 °C, and then scored on plates lacking histidine, with incubation at 30°. The 52 events were pooled from the 9 independent cultures.

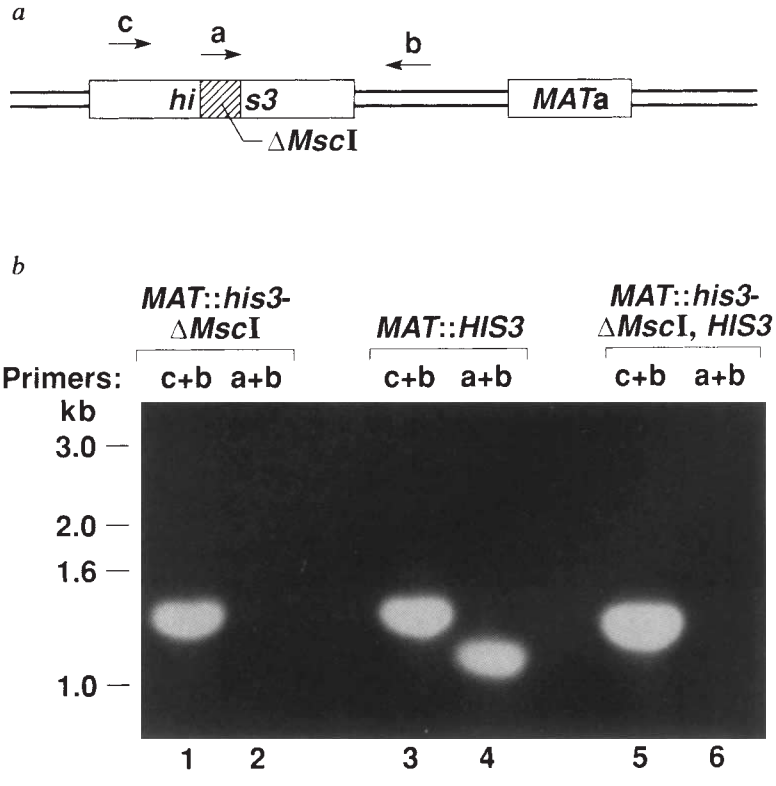

FIG. 2 A PCR-based assay to distinguish RNA-mediated gene conversions of homologous target sequences (*his3-ΔMscI*) from *HIS3* sequences inserted elsewhere. *a*, Structure of *his3-ΔMscI* on chromosome III and location of primers used for PCR. A 34-bp deletion (nucleotides 219–252; ref. 12) of the *his3* gene was constructed and inserted at *MAT*. This deletion spans the *MscI* site, the site of insertion of the artificial intron in plasmid *his3* sequences. *b*, Determination of the linkage between *HIS3* and *MAT*. The primers used for PCR are indicated above each lane. Lanes 1 and 2 show the starting parent strain YLD125. As expected no band is present with primers a and b. Lanes 3 and 4 shows a $His3^+$ prototroph linked to *MAT*. Lanes 5 and 6 show a chromosomal $His3^+$ prototroph, but the *HIS3* sequences have been inserted elsewhere in a region lacking *HIS3* homology.
METHODS. Linkage of *HIS3* and *MAT* was determined by PCR, following loss of the *GAL1-his3-AI* plasmid. Primer a, 5'-CATGCTCTGGCCAAGCATTCC (nucleotides 222–242, ref. 12) is complementary to sequences spanning the *MscI* site, deleted in *his3-ΔMcsI* and interrupted in plasmid *his3-AI* sequences. Primer b is complementary to *MAT* sequences 5'-CTGGGTAGAGTCTTATTGGCA (nucleotides 197379–197399; ref. 13). If *HIS3* is linked to *MAT*, then a 1-kb PCR product is expected. Primer c, 5'-CCCCGGCCGAATTCAGAGCA-GAAAGCCCTAGTA (nucleotides 27–47; ref. 12) was used in combination with primer b as a positive control. The conditions for PCR were: 3μl yeast DNA, 300 ng each primer, 200 μM dNTPs, and 2.5 units *Taq* polymerase (Perkin Elmer Cetus); with denaturation at 94 °C for 1 min, annealing at 55 °C for 1 min and extension at 72 °C for 2 min, for 25 cycles, followed by a 7 min extension at 72 °C. The validity of this PCR measurement was confirmed by Southern and genetic linkage analyses.

© 1993 Nature Publishing Group

Homologous insertion of cDNAs has two postulated effects: the removal of introns and the conversion of members of gene families[1,2]. For this process to have evolutionary significance, the RNA-mediated gene conversion event must occur in germ line cells. Participation of RNA in this evolutionary event requires that it be expressed and accessible for reverse transcription. Retroviruses can provide a vehicle for horizontal transmission of non-germline expressed transcripts. It has been shown that nonretroviral RNA is packaged, reverse-transcribed and integrated into the host genome[6,7]. Thus, RNA-mediated gene conversion could be important in germ-line substitutions, contributing to genome evolution, as well as somatic events. Kupiec has reported gene conversion of chromosomal Ty elements by Ty cDNA[8]. We have shown that gene conversion between a reverse transcript of a non-retroelement and its chromosomal allele occurs at an appreciable rate in *S. cerevisiae.* □

Received 14 September; accepted 12 November 1992.

1. Baltimore, D. *Cell* **40,** 481–482 (1985).
2. Fink, G. R. *Cell* **49,** 5–6 (1987).
3. Derr, L. K., Strathern, J. N. & Garfinkel, D. J. *Cell* **67,** 355–364 (1991).
4. Malone, R. E. *et al. Curr. Genet.* **14,** 211–223 (1988).
5. McGill, C. M. *et al. Curr. Genet.* **18,** 29–39 (1990).
6. Linial, M. *Cell* **49,** 93–102 (1987).
7. Dornburg, R. & Temin, H. M. *Molec. cell. Biol.* **8,** 2328–2334 (1988).
8. Melamed, C., Nevo, Y. & Kupiec, M. *Molec. cell. Biol.* **4,** 1613–1620 (1992).
9. Lea, D. E. & Coulson, C. A. *J. Genet,* **49,** 264–285 (1949).
10. Boeke, J. D., Lacroute, F. & Fink, G. R. *Molec. gen. Genet.* **197,** 345–346 (1984).
11. Alani, E., Cao, L. & Kleckner, N. *Genetics* **116,** 541–545 (1987).
12. Struhl, K. *Nucleic Acids Res.* **13,** 8587–8601 (1985).
13. Oliver, S. G. *et al. Nature* **357,** 38–46 (1992).

ACKNOWLEDGEMENTS. We thank B. Shafer for technical assistance and M. J. Curcio and S. L. Holbeck for critical evaluation of this manuscript. This work was supported in part by the National Cancer Institute, the DHHS with ABL and a Damon Runyon-Walter Winchell Cancer Research Fund Fellowship.

Arsenical-resistant trypanosomes lack an unusual adenosine transporter

Nicola S. Carter & Alan H. Fairlamb*

Department of Medical Parasitology, London School of Hygiene and Tropical Medicine, Keppel Street, London WC1E 7HT, UK

THE melaminophenyl arsenical melarsoprol is still used to treat African sleeping sickness[1–3], a disease caused by parasitic protozoa of the *Trypanosoma brucei* subgroup. Based on the observation that melamine antagonizes the trypanocidal activity of this class of drugs[4], we investigated whether other physiological compounds could compete for the same receptor. Here we report that the *in vitro* trypanolytic effect of melarsen oxide can be specifically abrogated by adenine, adenosine and dipyridamole, all of which compete for uptake by an adenosine transporter. Melarsen-sensitive trypanosomes have two high-affinity adenosine transport systems: a P1 type, which also transports inosine; and a P2 type, which also transports adenine and the melaminophenyl arsenicals. Melarsen-resistant trypanosomes lack P2 adenosine transport, suggesting that resistance to these arsenicals is due to loss of uptake.

As radiolabelled drug was unavailable, a direct approach towards identifying the mode of uptake and the intracellular targets for these drugs was not possible. Instead we used a simple spectrophotometric assay[5,6] to identify compounds that might antagonize the trypanolytic effect of arsenicals against bloodstream forms of *Trypanosoma brucei brucei.* Lysis by both melarsen oxide and phenylarsine oxide (which lacks the melamine ring and has no activity *in vivo*[7]) are dependent on both concentration and time with rapid lysis occurring at concentrations greater than 0.5 μM (Fig. 1*a* and *b*). Compounds were screened at a 100-fold excess (50 μM) for their ability to block lysis. These included a selection of basic amino acids, polyamines, nitrogen-containing vitamins and coenzymes, and the commonly occurring purines and pyrimidines and their nucleotides. Of the 32 compounds tested, only the purines, adenine and adenosine, were able to significantly delay lysis by melarsen oxide in a dose-dependent manner (Fig. 1*c* and *e*). In sharp contrast, addition of these purines in up to a 100-fold excess had no effect on lysis induced by phenylarsine oxide (Fig. 1*d* and *f*). Dipyridamole, a general nucleoside transport inhibitor[8,9], was also a potent inhibitor of melarsen oxide-induced lysis, but again had no effect on phenylarsine oxide-induced lysis (Fig. 1*g* and *h*).

TABLE 1 Effects of 1 mM inosine on adenosine transport in a melarsen sensitive and resistant *Trypanosoma brucei brucei* cloned line

Phenotype	Uptake (pmol/10^8 cells/sec) No inosine (P1 and P2)	+1 mM inosine (P2 only)	Net (residual P1)
Sensitive	10.7 ± 1.1 (6)	4.7 ± 0.5 (6)	6.0
Resistant	1.9 ± 0.3 (5)	ND (6)	1.9

Transport was measured with 1 μM [^{3}H]adenosine (final specific activity, 0.56 Ci mmol^{-1}) at 25 °C in the presence (P1-inhibited) or absence of 1 mM inosine as described for Fig. 3, in two cloned lines of *Trypanosoma brucei brucei,* the parent S427 c118 (ref. 32), which is susceptible to melaminophenyl arsenicals, and a derived melarsen-resistant line S427 cRU15 (ref. 6). Results are expressed as a mean value (number of determinations given in brackets) plus or minus standard error of the mean. ND, No detectable rate could be measured and regression coefficients were 0.67 or less.

As the Trypanosomatidae have no *de novo* synthesis of purines and instead salvage pre-formed purines from the host[10,11] we investigated whether this receptor could be part of an adenine/adenosine carrier by measuring [^{3}H]adenosine transport into the trypanosome. As uptake was extremely rapid, transport kinetics were measured at 1-second intervals over the first five seconds, and initial rates were determined by linear regression analysis. As detailed below, we can identify two distinct adenosine transporters in *T. brucei,* consistent with earlier observations in other Trypanosomatidae[9,12,13]. For convenience we have named these transport systems P1 and P2 (Fig. 2). Uptake of 1 μM adenosine via the P1-transporter can be inhibited in a dose-dependent and saturable manner by inosine, accounting for 60–70% of total adenosine uptake (Fig. 3*a*, open symbols). Likewise, uptake of adenosine via the P2 transporter can be inhibited by increasing concentrations of adenine, accounting for 30–40% of total adenosine uptake into the cell (Fig. 3*b*, open symbols). When saturating concentrations of both adenine and inosine are present, adenosine transport is completely inhibited (Fig. 3*a* and *b*, closed symbols).

By saturating one transporter with either 1 mM inosine (P1) or 100 μM adenine (P2), the kinetic parameters for [^{3}H]adenosine uptake of either transporter can be shown to obey simple Michaelis–Menten kinetics (Fig. 3*c* and *d*). The apparent K_m values for the P1 and P2 transporters are 0.15 ± 0.02 and 0.59 ± 0.05 μM, respectively, with V_{max} values of 10.60 ± 0.53 and 9.5 ± 0.27 pmol per 10^8 cells per second, respectively. As expected, adenine competitively inhibits adenosine transport on the P2 transporter with a K_i of 0.38 μM (Fig. 3*e*). Moreover, the P2, but not the P1 transporter can be markedly inhibited by 1 μM melarsen oxide or melarsoprol (not shown). In the case of melarsoprol, kinetic analysis shows competitive-type inhibition with a K_i of 0.28 μM (Fig. 3*f*). Nucleoside transporters in other Trypanosomatidae[14–16] and in mammalian cell types[8] usually have a broad substrate specificity, transporting both

* To whom correspondence should be addressed.

© 1993 Nature Publishing Group